Fractal analysis of zona pellucida thickness: bending energy as a predictive window on day 2 embryo fate

M. S. Bezerra Espinola[1] C. Aragona[1], A. Linari[2], G. Micara[2], D. Tranquilli[2], B. Visconti[3], A. Giuliani[4], M. Bizzarri[5]

[1]Systems Biology Group, "Sapienza" University of Rome, Rome, Italy
[2]Department Maternal Infantile and Urogynecological Sciences, Infertility and Assisted Reproduction Unit, "Sapienza" University of Rome, Rome, Italy
[3]Faculty of Medicine, University Tor Vergata, Rome, Italy
[4]Department of Environment and Health, Istituto Superiore di Sanità, Rome, Italy
[5]Department of Experimental Medicine, "Sapienza" University of Rome, Systems Biology Group, Rome, Italy

ABSTRACT — OBJECTIVE: *The quality of the embryo is crucial for the outcome of in vitro fertilization; however, the ability to accurately distinguish embryos with the highest reproductive potential from others is not entirely reliable. Most of the methods of classification of embryos in Assisted Reproductive Technologies (ART) are subjective and in clinical practice, there is still a lack of semi or fully automated procedures. Since measurement of Zona Pellucida Thickness Variability is a reliable parameter for assessing the embryo's hatching capacity, we describe a new automatic method to record and quantify a new morphological parameter, the Local Zona Pellucida Thickness Variation (LZPTV) using an innovative fractal-based analysis similar to Bending Energy that captures the high-frequency variability of the thickness of the Zona Pellucida.*

PATIENTS AND METHODS: *436 digitized images of embryos obtained from 187 Intracytoplasmic Sperm Injection (ICSI) procedures, were evaluated retrospectively. The images of the embryos classified according to Veeck's Embryo Grading Classification (VEGC) were processed by the software program "Embryon" for LZPTV computation.*

RESULTS: *Patients with high LZPTV embryos had a significantly higher birth rate (54.7%) than patients with low LZPTV embryos (9.7%), or patients with Grade I VEGC (33.7%), the LZPTV measure also had a significantly higher specificity than the VEGC to predict pregnancy (83.5% vs. 53.8%) or delivery (80.2% vs. 49.1%).*

CONCLUSIONS: *This new parameter, therefore, provides a reliable additional source of information that could be included in an integrative standardized approach in ART practice and research.*

KEYWORDS
Zona pellucida thickness, Bending energy, Fractal analysis, Embryo quality.

Corresponding Author
Maria Salome Bezerra Espinola, PhD; e-mail: espinolasalome@gmail.com

DOI: 10.32113/ijmdat_20217_341

INTRODUCTION

Infertility is a social problem because it raises issues relating to the health and well-being of individuals, couples, and society as a whole[1,2]. The medical treatment of infertility has progressed dramatically, making parenting possible for many who until recently would not been able to achieve this goal. Multiple pregnancy, however, resulting from the transfer of multiple embryos, together with high-risk maternal and perinatal adverse conditions, are significant limitations of Assisted Reproductive Technologies (ART). Successful single embryo transfer remains the "golden standard"[3,4] still not reached.

A series of morphological, morphokinetics, automated and semi-automated non-invasive methodologies also based on Artificial Intelligence has been developed to evaluate the feasibility of a human embryo to be implanted in a woman uterus but, to date, none has been proven superior to the others[5-21].

Criteria that can be assessed by routine microscopy prior to fertilization or embryo transfer would be helpful in selecting embryos for transfer during ART procedures. However, very few reliable, predictive and non-invasive markers have been identified so far. An important prognostic parameter for evaluating the success of an *in vitro* fertilization treatment is the thickness variation of the Zona Pellucida (ZP). The Thickness of the Zona Pellucida (ZPT) and the Variability of the Thickness of the Zona Pellucida (ZPTV) seem to successfully predict the clinical outcome of ART[22-33]. However, semi or fully automated methods using these parameters are lacking due to the significant variability inter-operators. One of the major problems with subjective evaluation and selection is that it cannot be considered robust and reliable and does not provide predictive clinical information[5-8,18].

It is also important to evaluate the morphological criteria in the measurement of the variation in the thickness of the ZP which can be carried out with the aid of a digitized imaging system and analysis software.

To be suitable for larger clinical studies, an automated procedure must evaluate the morphology of the shape with quantitative and reproducible methods[31-35].

The aim of the present research was: 1) to evaluate the clinical efficacy of an original quantitative morphological analysis of ZP in digitized embryos collected on Day 2 after Intracytoplasmic Sperm Injection (ICSI); 2) to evaluate the predictive potential of this method on the fate of the embryo with respect to the Veeck's Embryo Grading Classification (VEGC) widely used for the assessment of embryo quality[9].

This new method, developed by "Embryon" software program, allows to characterize the morphology of Zona Pellucida of the embryo with a single numerical value the Local Zona Pellucida Variation (LZPTV), a morphological descriptor related to the Bending Energy of the embryo Zona Pellucida Thickness (ZPT).

PATIENTS AND METHODS

Clinical selection of patients and ICSI procedures

The material was retrospectively taken from 2 data sets of the Infertility and Assisted Reproduction Unit, Department of Obstetrics and Gynecology, "Sapienza" University of Rome (Italy) in October 2011-October 2012 with strict adherence to the highest Italian Ethical and legal requirements and with formal approval of the Institutional Ethics Committee for the research article (prot. N. 807/12), including full informed consent and no selection of embryos. Data set 1 (algorithm training data set) included 66 images from 30 consecutive ICSI procedures. Data set 2 (algorithm test data set) included 370 images from another 157 consecutive ICSI procedures.

The age of the female patients ranged from 25 to 45 years (mean ± SD = 36.5 ± 4.7 years); the age of the male patients ranged from 30 to 51 years (mean ± SD = 39.68±4.8 years).

All patients underwent a standard primary infertility assessment. They had previous failed *in-vitro* fertilization (IVF) treatments ranging from 0 to 4. All female patients had normal basal FSH and estradiol values and normal thyroid function[36]. ICSI treatment management was performed as already reported[37].

Preparation of semen samples collected by masturbation was performed following the World Health Organization (WHO) standard protocol[38]. ICSI was performed on methaphase II oocytes according to the procedure reported by Palermo [39]. Oocyte fertilization was assessed 16-18 hours after ICSI and confirmed by the presence of two pronuclei. Embryos were observed by an inverted microscope with Hoffman modulation contrast at 400x (TE 2000 U, Nikon Corporation, Tokyo, Japan) evaluated according to the amount of fragmentation and the number of blastomeres and routinely scored using the VEGC (I, II, III, IV, or V) at 40-42 hours after ICSI[9]. All images were captured by a computerized system (X-Pro™ Alexasoft, Nikon Instruments, Florence, Italy).

Embryo transfer was performed at Day 2 after oocytes retrieval under US guidance, with the Wallace embryo transfer catheter (HG Wallace®, Hythe, Kent, UK) by the same doctor to avoid the variability inter-operators. All patients received supplemental Progesterone (50 mg/day, intramuscular (i.m.); Prontogest®; IBSA, Lodi, Italy) from the day of replacement[37].

Chemical pregnancy was initially determined 14 days after embryo transfer by a positive qualitative serum β-hCG assay, followed by repeated quantitative β-hCG levels. Clinical pregnancy was defined as at least one fetus with a positive heartbeat revealed by transvaginal sonography 4 to 5 weeks after embryo transfer [37]. The Implantation Rate (IR) was defined as the number of gestational sacs on US as a percentage (%) of embryos transferred.

Image processing

The images obtained in format jpg with a resolution of 2560 x 1920 or 1280 x 960 pixels were processed by the "Embryon" software program (Advanced Computer Systems, ACS, Rome, Italy). Embryo images were segmented to highlight the ZP region, leading to the identification of the outer and inner boundaries of the ZP (Figure 1). This segmentation method is based on an active contour parametric model adapted to the ZP segmentation of human embryo images[40,41]. The active contour (or snake) method[42] is widely used for segmentation of medical image, due to its ability to segment diffuse contours with low intensity values. This feature was used for our purposes in the present study. ZP is relatively transparent and does not have a high contrast outer boundary, even at the early embryonic stages. Furthermore, human embryos may have some artifacts, removed by morphological operations on the edge as outlined by Morales et al[12,43]. The active contour is manually initialized if the automatic segmentation process fails, allowing ZP boundaries to be correctly identified even in the most difficult circumstances.

The external and internal boundaries of the ZP were identified by a polygon A and B respectively, which, in turn, were defined by a set of reference points along the ZP boundaries indicated as points in Figure 1.

Following the detection of the internal and external profiles of the ZP boundaries, the ZP was analyzed by calculating a new morphological parameter, the LZPTV related to the variability of the ZPT.

Morphological parameters: mathematical considerations

The LZPTV method was based on the application of an innovative analysis of the internal and external boundaries of the ZP, which considers the local "curvature" of the ZP boundaries.

The first step in calculating the LZPTV is to accurately determine the ZPT defined as the distance between the reference points along the outer and inner ZP boundaries respectively.

As shown in Figure 1, the distance ZPT between the polygons **A** and **B** is calculated as the length of a segment **z** on the half-line **s**, originating in the barycenter **c** of the inner polygon **B** and passing through the reference point **Ri**, between the internal polygon **B** and the outer polygon **A**.

This set of distances, i.e. the lengths of the segments **zi,** are subsequently used to construct, in a Cartesian plane in polar coordinates, a broken line representing the set of distances as an angular parameter **βi** defined for each point **Ri** as the angle comprised between the half-line **s**, passing for the barycenter **c** and the point **Ri**, and a reference line **r** passing for the barycenter **c**. The broken line is therefore a sequence of N segments, each between two successive points **pi** in the Cartesian plane, and which will have a number **N** of vertexes **v** corresponding to the number of the same points **pi** as shown in Figure 1.

At each vertex **vi** a local curvature is calculated, by using the broken line points within a neighborhood of the given vertex. The final result of this operation is a set of local curvature **k(i)**, which is used to calculate the final LZPTV shape factor using the following formula:

$$LZPTV = (L^2 / N)\sum_{i=0}^{N-1} k(i)^2$$

where **L** is the length of the broken line and **N** is the number of vertices. The number **N** of reference points **Ri** (with **i** varying from 1 to N) can vary very much, and it is clear that the greater their number, more details of the ZPT variations will be captured by LZPTV morphological parameter. However, the LZPTV remains constant as

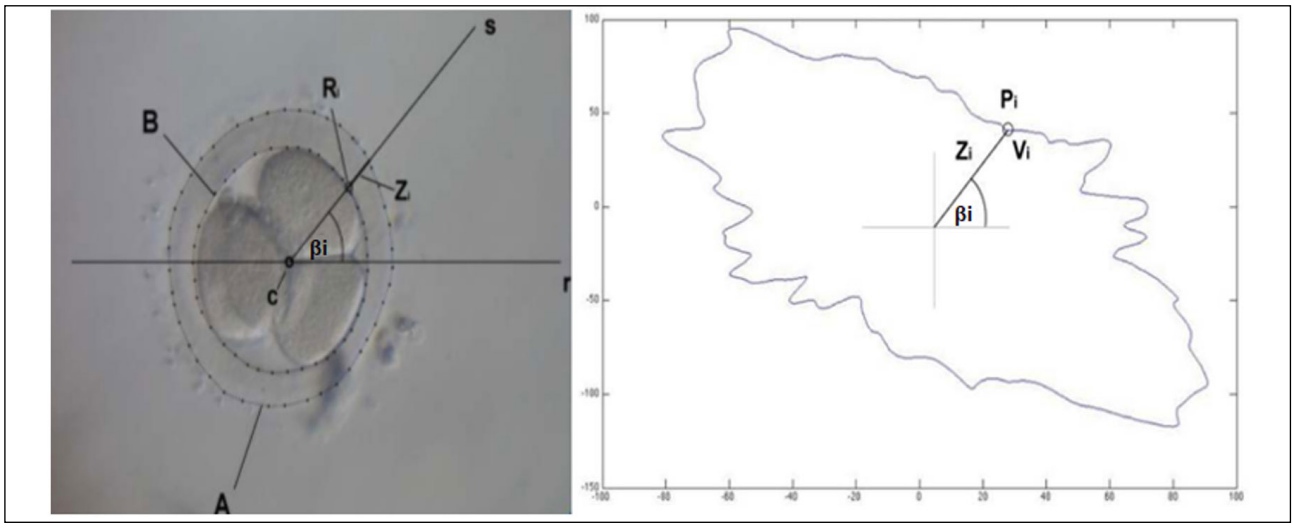

Figure 1. Zona pellucida boundaries and corresponding thickness curve.

the number of points increases behond a threshold value of N=10000, corresponding to the maximum level of details captured by the imaging system used. LZPTV is conceptually related to the Normalized-Bending Energy (NBE) of the ZPT curve, since the shape changes are the expression of the amount of energy needed to transform the specific shape being analyzed into its lowest energy state (i.e., a circle)[44].

LZPTV/NBE represents a means of obtaining quantitative information on the complexity of shapes under investigation. For biological shapes, Normalized-Bending Energy (NBE) indeed provides a particularly significant physical interpretation in terms of the energy to be applied in order to produce or modify specific objects[45]. Seemingly, the LZPTV parameter expresses the variation measured as a function of the ideal curvature expected for an object in the shape of a perfect circle, although the difference recorded represents a true geometric modification and should be considered as a true morphological index. In systems biology, both NBE and LZPTV methods are described as reliable indicators of shape changes, phenotypic transition, and cancer cell behavior[46,47].

The LZPTV parameter (including the segmentation of the outer and inner boundaries ZP) was then processed by "Embryon". All LZPTV computations were performed blindly.

Algorithm training set

Embryos with LZPTV values above an identified threshold value were classified "Top", while LZPTV values below this value were labeled as "Poor". According to the classification of individual embryos, the diagnostic test of a treatment is defined as follows: "Top" treatment, if at least one "Top" embryo was present; "Poor" treatment, if no "Top" treatment was present. In this regard an optimal LZPTV threshold was experimentally determined on a training data set of 66 images, obtained from the first 30 consecutive ICSI procedures. The classical method based on Receiver Operating Characteristic (ROC) curve analysis was used. More precisely, the optimal threshold of 18.5 x 10^3 was determined using the Youden index criteria[48].

As a consequence of the Italian Law, that explicitly prohibits the selection of embryos, we could not train our pattern recognition algorithm based on the characteristics of individual

embryos, and we had to rely on indirect evidence based on multiple transfers. Therefore, the 'independent statistical units' were the transfers made from one, two or three embryos. We therefore adopted a most conservative approach considering as "Poor" a transfer made by three "morphologically poor" embryos, and as "Top", a transfer in which at least one embryo is Top. This choice determines an underestimation of the accuracy of the precision because in the 2Poor-1Top (by far the most frequent "Top" configuration), only one out of three embryos met the optimality criteria.

Statistical Analysis

Data were collected and analyzed retrospectively by calculating statistical tests with estimated population midpoints and 95% confidence interval (CI). The CIs are calculated according to the efficient (corrected for continuity) score method described by Newcombe[49]. The statistical parameters commonly used to characterize the accuracy of diagnostic tests were sensitivity, specificity, Positive Predictive Value (PPV), Negative Predictive Value (NPV) and prevalence.

RESULTS

According to LZPTV analysis, the 370 embryos were classified as: 62 "Top" embryos and 308 "Poor" embryos. The 157 patients were divided in "Top" and "Poor" clusters: "Top" (Group A = 54 patients) if at least one "Top" embryo was present; "Poor" (Group B = 103 patients) if not even one Top embryo was present.

According to VEGC, the same 370 embryos were classified as: 142 "Grade I", 158 "Grade II", 62 "Grade III", 7 "Grade IV" and 1 "Grade V". The same 157 patients were divided in "Grade I" and "Grade II-V" clusters: "Grade I" (Group C = 89 patients) if at least one "Grade I" embryo was present; "Grade II-V" (Group D = 68 patients) in all other cases. In Group A, B, C and D, mean age (years) were 36.7, 36.4, 36.3 and 36.7 while mean number of embryos transferred were 2.5, 2.3, 2.4, and 2.3 respectively (with 2.4 the overall mean number of embryos transferred).

Clinical outcomes for the four different groups are indicated in Table I. Group A "Top" embryos had 57.4% of birth compared to 9.7% for the Group B "Poor" embryos ($p < 0.05$). Similar results hold for the pregnancy rate - 72.2% of Group A *vs.* 26.2% of Group B ($p < 0.05$) - and for the implantation rate (IR) – 36.6% of Group A *vs.* 13,1% of Group B ($p < 0.05$). Moreover, the IR of Group A was significantly better than the overall IR ($p < 0.05$).

On the contrary, in the case of the standard VEGC method the birth rate of Group C "Grade I" was 33.7%, not statistically different from 16.2% for the Group D "Grade II-V" and the IR of Group C was not significantly better than the overall IR.

Furthermore, according to Table II and Table III, LPZTV parameter had a statistical significantly higher specificity than the VEGC in predicting pregnancy (83.5% *vs.* 53.8%; $p < 0.05$) and birth (80.2% *vs.* 49.1%; $p < 0.05$). The two diagnostic measures were not significantly different with regard to sensitivity, either for pregnancy or for the delivery end-point. In other words, the LZPTV method introduced significantly fewer false-positive cases for embryo transfer and proved to be a significantly more selective and reliable indicator than the Veeck's classification.

Table I. Clinical outcomes in LZPTV and VEGC patients.

	LZPTV						VEGC			
	Total		Group A		Group B		Group C		Group D	
	N	%	N	%	N	%	n	%	N	%
Patients	157	100.0	54	100.0	103	100.0	89	100.0	68	100.0
Not Pregnancy	91	58.0	15	27.8	76	73.8	42	47.2	49	72.1
Pregnancy	66	42.0	39	72.2	27	26.2	47	52.8	19	27.9
Abortion	25	15.9	8	14.8	17	16.5	17	19.1	8	11.8
Birth	41	26.1	31	57.4	10	9.7	30	33.7	11	16.2
Embryos Transferred	370	100.0	134	100.0	236	100.0	215	100.0	155	100,0
Embryos Implanted	80	21.6	49	36.6	31	13.1	59	27.4	21	13.5

Table II. Statistical analysis of LZPTV, VEGC or Combined tests in predicting pregnancy.

Pregnancy rate	%	CI (%)				
	42.0	34.3 – 50.2				
	LZPTV		VEGC		Combination	
	%	CI (%)	%	CI (%)	%	CI (%)
Sensitivity	59.1	46.3 - 70.8	71.2	58.6 - 81.4	87.9	77.0 - 94.2
Specificity	83.5	74.0 - 90.1	53.8	43.1 - 64.2	49.4	38.9 - 60.1
PPV	72.2	58.1 - 83.1	52.8	42.0 - 63.4	55.8	45.7 - 65.4
NPV	73.8	64.0 - 81.7	72.1	59.7 - 81.9	84.9	71.8 - 92.8

The use of Grade I as marker for the expected positive outcome, was dictated by the fact that using Grade I-II as prediction criterion practically abolishes the specificity of the test with vast majority of the embryos predicted as "viable".

An indirect, albeit relevant, evidence of the advantage of the LZPTV method is the fact the overall probability of birth is 26.1% (CI 19.6% - 33.8%), significantly lower than the birth rate of the LZPTV group "Top" which is equal to 57.4% (CI 43.3% - 70.5%). On the other hand, the probability of birth of the grade I Veeck's group was 33.7% (CI 24.2% - 44.6%), not significantly different from probability of 26.1% (CI 19.6% - 33.8%) of the total population (Table III). The same consideration also applies to pregnancy (Table II).

A crucial point to be addressed is the relationship between LZPTV and VEGC. The significant correlation (p = 0.0064, Fisher's exact test) between LZPTV and VEGC (Table IV) suggests that both parameters refer to the same phenomenon and can be assumed to share the same biological basis. Indeed, the percentage of embryos giving consistent results (Top/Grade I and Poor/Grade II-V) for both parameters is around 60% but LZPTV gives a more reliable viability measure. The correlation between LZPTV and Veeck classification methods makes the combined use of the two approaches unnecessary, because Veeck classification does not add any relevant independent information in improving the predictive capability of LZPTV as reported in Table II and Table III.

Table III. Statistical analysis of LZPTV, VEGC or Combined tests in predicting birth.

Pregnancy rate	%	CI (%)				
	42.0	34.3 – 50.2				
	LZPTV		VEGC		Combination	
	%	CI (%)	%	CI (%)	%	CI (%)
Sensitivity	75.6	59.4 - 87.1	73.2	56.8 - 85.2	97.6	85.6 - 99.9
Specificity	80.2	71.5 - 86.8	49.1	39.8 - 58.5	44.8	35.7 - 54.3
PPV	57.4	43.3 - 70.5	33.7	24.2 - 44.6	38.5	29.2 - 48.5
NPV	90.3	82.5 - 95.7	83.8	72.5 - 91.3	98.1	88.6 - 99.9

Table IV. LZPTV vs. VEGC patients contingency table.

	VEGC	
LZPTV	**Grade I**	**Grade II-V**
Top	39	15
Poor	50	53

DISCUSSION

In the present study, we have shown that a quantitative morphological analysis of the ICSI embryo shape on day 2 can provide an additional reliable source of information in ART. This method allows the detection of higher quality embryos with greater ability to proceed to term. The proposed method is based on the calculation of a "form factor", linked to the local morphological variability of the ZP embryo, rather than to its macroscopic characteristics. Some other similar methods (e.g. ZPTV) focus only on the high-level mean ZP value of the shape, while our approach analyzes a well-defined, granular set of local form factors measured near the ZP boundaries. Our method is based on the application of harmonic analysis techniques in the frequency-domain representation of the ZP boundaries. This methodology allows the characterization of local morphological ZP variability of embryos by providing a dimensionless, and scale-invariant parameter. We think this parameter is closely linked to the quality of the embryo. Embryos with high LZPTV values indeed have higher implantation capacities, and a greater likelihood of proceeding to term than those selected with the widely accepted Veeck embryo scoring method.

VEGC of embryos confirmed good reliability in the present study. However, although no difference was found between the "Top" embryos group and grade I embryos group in terms of clinical outcome, the LZPTV measure provided significant higher specificity with respect to both pregnancy and birth rates.

CONCLUSIONS

LZPTV measurement appears as a tool that can be used to select embryos for transfer on Day 2 after fertilization providing a new and accurate assessment of higher quality embryos. Furthermore, this criterion appears to be even more important when the embryos of suboptimal morphology are available for transfer.

These observations, whether confirmed in larger series and possibly in blastocysts, may provide useful criteria in a policy of single embryo transfer.

Acknowledgments:
We would like to thank Advanced Computer Systems S.p.A. Rome, Italy for providing "Embryon" software program and Dr Luca Galli and Dr Davide Passaro for the competent technical assistance in the use of the software program.

Funding:
No funding is declared for this article.

Conflict of Interest:
The authors declare that there are no conflicts of interest.

References

1. Malina A, Błaszkiewicz A, Owczarz U. Psychosocial aspects of infertility and its treatment. Ginekol Pol 2016; 87: 527-531.
2. Royani Z, Heidari M, Vatanparast M, Yaghmaei F, Sarcheshme AK, Majomerd JK. Predictors of quality of life in infertile couples. J Menopausal Med 2019; 25: 35-40.
3. Adamson GD, Norman RJ. Why are multiple pregnancy rates and single embryo transfer rates so different globally, and what do we do about it? Fertil Steril 2020; 114: 680-689.
4. Tiitinen A. Single embryo transfer: why and how to identify the embryo with the best developmental potential. Best Pract Res Clin Endocrinol Metab 2019; 33: 77-88.
5. Cummins JM, Breen TM, Harrison KL, Shaw JM, Wilson LM, Hennessey JF. A formula for scoring human embryo growth rates in in vitro fertilization: its value in predicting pregnancy and in comparison with visual estimates of embryo quality. J In Vitro Fert Embryo Transf 1986; 3: 284-295.
6. Magdi Y, Samy A, Abbas AM, Ibrahim MA, Edris Y, El-Gohary A, Fathi AM, Fawzy M. Effect of embryo selection based morphokinetics on IVF/ICSI outcomes: evidence from a systematic review and meta-analysis of randomized controlled trials. Arch Gynecol Obstet 2019; 300:1479-1490.
7. Louis CM, Erwin A, Handayani N, Polim AA, Boediono A, Sini I. Review of computer vision application in in vitro fertilization: the application of deep learning-based computer vision technology in the world of IVF. J Assist Reprod Genet 2021 Apr 3. doi: 10.1007/s10815-021-02123-2. Epub ahead of print.
8. Zaninovic N, Rosenwaks Z. Artificial intelligence in human in vitro fertilization and embryology. Fertil Steril 2020; 114: 914-920.
9. Veeck LL. Oocyte assessment and biological performance. Ann N Y Acad Sci 1988; 541: 259-274.
10. Scott LA, Alvero R, Leondires M, Miller BT. The morphology of human pronuclear embryos is positively related to blastocyst development and implantation. Hum Reprod 2000; 15: 2394-2403.
11. Gianaroli L, Magli MC, Ferraretti AP, Fortini D, Greco N. Pronuclear morphology and chromosomal abnormalities as scoring criteria for embryo selection. Fertil Steril 2003; 80: 341-349.
12. Morales DA, Bengoetxea E, Larrañaga P. Automatic segmentation of zona pellucida in human embryo images applying an active contour model. In: 12th Annual Conference on Medical Image Understanding and Analysis 2008; pp. 209-213.
13. Molina I, Martínez JV, Pertusa JF, Balasch S, Iniesta I, Pellicer A. Assessment of the implantation of day-2 human embryos by morphometric nonsubjective parameters. Fertil Steril 2014; 102: 1022-1028.
14. Akamine K, Mekaru K, Gibo K, Nagata C, Oishi S, Miyagi M, Heshiki C, Kinjo T, Masamoto H, Aoki Y. Comparative study of obstetric and neonatal outcomes of live births between poor- and good-quality embryo transfers. Reprod Med Biol 2018; 17: 188-194.

15. Ziebe S, Petersen K, Lindenberg S, Andersen AG, Gabrielsen A, Andersen AN. Embryo morphology or cleavage stage: how to select the best embryos for transfer after in-vitro fertilization. Hum Reprod 1997; 12: 1545-1549.
16. Coello A, Meseguer M, Galán A, Alegre L, Remohí J, Cobo A. Analysis of the morphological dynamics of blastocysts after vitrification/warming: defining new predictive variables of implantation. Fertil Steril 2017; 108: 659-666.
17. Molina I, Lázaro-Ibáñez E, Pertusa J, Debón A, Martínez-Sanchís JV, Pellicer A. A minimally invasive methodology based on morphometric parameters for day 2 embryo quality assessment. Reprod Biomed Online 2014; 29: 470-480.
18. Sigalos GA, Triantafyllidou O, Vlahos NF. Novel embryo selection techniques to increase embryo implantation in IVF attempts. Arch Gynecol Obstet 2016; 294: 1117-1124.
19. Lundin K, Park H. Time-lapse technology for embryo culture and selection. Ups J Med Sci 2020; 125: 77-84.
20. Santos Filho E, Noble JA, Poli M, Griffiths T, Emerson G, Wells D. A method for semi-automatic grading of human blastocyst microscope images. Hum Reprod 2012; 27: 2641-2648.
21. Matchtinger R, Racowsky C. Morphological systems of human embryo assessment and clinical evidence. Reprod Biomed Online 2013; 26: 210-221.
22. Familiari G, Nottola SA, Micara G, Aragona C, Motta PM. Is the sperm-binding capability of the zona pellucida linked to its surface structure? A scanning electron microscopic study of human in vitro fertilization. J In Vitro Fert Embryo Transf 1988; 5: 134-143.
23. Familiari G, Nottola SA, Micara G, Aragona C, Motta PM. Human in vitro fertilization: the fine three-dimensional architecture of the zona pellucida. Prog Clin Biol Res 1989; 296: 335-344.
24. Familiari G, Nottola SA, Macchiarelli G, Micara G, Aragona C, Motta PM. Human zona pellucida during in vitro fertilization: an ultrastructural study using saponin, ruthenium red, and osmium-thiocarbohidrazide. Mol Reprod Dev 1992; 32: 51-61.
25. Garside WT, Loret de Mola JR, Bucci JA, Tureck RW, Heyner S. Sequential analysis of zona thickness during in vitro culture of human zygotes: correlation with embryo quality, age, and implantation. Mol Reprod Dev 1997; 47: 99-104.
26. Palmstierna M, Murkes D, Csemiczky G, Andersson O, Wramsby H. Zona pellucida thickness variation and occurrence of visible mononucleated blastomers in preembryos are associated with a high pregnancy rate in IVF treatment. J Assist Reprod Genet 1998; 15: 70-75.
27. Gabrielsen A, Lindenberg S, Petersen K. The impact of the zona pellucida thickness variation of human embryos on pregnancy outcome in relation to suboptimal embryo development. A prospective randomized controlled study. Hum Reprod 2001; 16: 2166-2170.
28. Nottola SA, Makabe S, Stallone T, Familiari G, Correr S, Macchiarelli G. Surface morphology of the zona pellucida surrounding human blastocysts obtained after in vitro fertilization. Arch Histol Cytol 2005; 68: 133-141.
29. Sun YP, Xu Y, Cao T, Su YC, Guo YH. Zona pellucida thickness and clinical pregnancy outcome following in vitro fertilization. Intern J Gynec Obs 2005; 89: 258-262.
30. Gabrielsen A, Bhatnager PR, Petersen K, Lindenberg S. Influence of zona pellucida thickness of human embryos on clinical pregnancy outcome following in vitro fertilization treatment. J Assist Reprod Genet. 2000; 17: 323-328
31. Bizzarri M, Pasqualato A, Cucina A, Pasta V. Physical forces and non linear dynamics mould fractal cell shape: quantitative morphological parameters and cell phenotype. Histol Histopathol 2013; 28: 155-174.
32. Bizzarri M, Palombo A, Cucina A. Theoretical aspects of systems biology. Prog Biophys Mol Biol 2013; 112: 33-43.
33. Ingber D. How cells (might) sense microgravity. FASEB J 1999; 13: S3-15.
34. Bizzarri M, Giuliani A, Cucina A, D'Anselmi F, Soto AM, Sonnenschein C. Fractal analysis in a systems biology approach to cancer. Semin Cancer Biol 2011; 21: 175-182.
35. Fitzgibbon A, Pilu M, Fisher RB. Direct least square fitting of ellipses. IEEE Trans Pattern Anal Machine Intell 1999; 21: 476-480.
36. Fumarola A, Grani G, Romanzi D, Del Sordo M, Bianchini M, Aragona A, Tranquilli D, Aragona C. Thyroid function in infertile patients undergoing assisted reproduction. Am J Reprod Immunol 2013; 70: 336-341.
37. Mohamed MA, Sbracia M, Pacchiarotti A, Micara G, Linari A, Tranquilli D, Espinola SM, Aragona C. Urinary follicle-stimulating hormone (FSH) is more effective than recombinant FSH in older women in a controlled randomized study. Fertil Steril 2006; 85: 1398-1403.
38. World Health Organization. WHO laboratory manual for the examination and processing of human semen. Fifth Edition. Geneva: WHO Press; 2010.
39. Palermo G, Joris H, Devroey P, Van Steirteghem AC. Pregnancies after intracytoplasmic injection of single spermatozoon into an oocyte. Lancet 1992; 4: 17-18.
40. Boscolo R, Brown MS, McMitt-Gray MF. Medical image segmentation with knowledge-guided robust active contours. Radiographics 2002; 22: 437-438.
41. Giusti A, Giorgio C, Gambardella L, Magli M, Gianaroli L. "Segmentation of Human Zygotes in Hoffman Modulation Contrast Images 2009.
42. Kass M, Witkin A, Terzopoulos D. Snake: Active contour models. Int J Comp Vis 1998; 1: 321-331.
43. Morales DA, Bengoetxea E, Larranaga P. Selection of human embryos for transfer by Bayesian classifiers. Comput Biol Med 2008; 38: 1177-1186.
44. Bowie JE, Young IT. An analysis technique for biological shape-III. Acta Cytol 1977; 21: 739-746.
45. Castleman KR. Digital image processing. Prentice Hall, Englewood Cliffs 1996.
46. Dinicola S, D'Anselmi F, Pasqualato A, Proietti S, Lisi E, Cucina A, Bizzarri M. A systems biology approach to cancer: fractals, attractors, and nonlinear dynamics. OMICS 2011; 15: 93-104.
47. D'Anselmi F, Valerio M, Cucina A, Galli L, Proietti S, Dinicola S, Pasqualato A, Manetti C, Ricci G, Giuliani A, Bizzarri M. Metabolism and shape in cancer: a fractal analysis. Int J Biochem Cell Biol 2011; 43: 1052-1058.
48. Fluss R, Faraggi D, Reiser B. Estimation of the Youden Index and its associated cutoff point. Biom J 2005; 47: 458-472.
49. Newcombe RG. Two-sided confidence intervals for the single proportion: comparison of seven methods. Stat Med 1998; 17: 857-872.